Clinical Chemistry 68:7
917–926 (2022)

Jagged Ends on Multinucleosomal Cell-Free DNA Serve as a Biomarker for Nuclease Activity and Systemic Lupus Erythematosus

Spencer C. Ding [a,b,c,†] Rebecca W.Y. Chan,[a,b,c,†] Wenlei Peng,[a,b,c] Liangbo Huang,[a,b,c] Ze Zhou,[a,b,c] Xi Hu,[a,b,c] Stefano Volpi,[d,e] Linda T. Hiraki [f] Augusto Vaglio,[g,h,i] Paride Fenaroli,[j] Paola Bocca,[d] Lai-Shan Tam [k] Priscilla C.H. Wong,[k] Lydia H.P. Tam,[k] Peiyong Jiang [a,b,c] Rossa W.K. Chiu,[a,b,c] K.C. Allen Chan [a,b,c,l] and Y.M. Dennis Lo[a,b,c,l,*]

BACKGROUND: Jagged ends of plasma DNA are a recently recognized class of fragmentomic markers for cell-free DNA, reflecting the activity of nucleases. A number of recent studies have also highlighted the importance of jagged ends in the context of pregnancy and oncology. However, knowledge regarding the generation of jagged ends is incomplete.

METHODS: Jaggedness of plasma DNA was analyzed based on Jag-seq, which utilized the differential methylation signals introduced by the DNA end-repair process. We investigated the jagged ends in plasma DNA using mouse models by deleting the *deoxyribonuclease 1* (*Dnase1*), *DNA fragmentation factor subunit beta* (*Dffb*), or *deoxyribonuclease 1 like 3* (*Dnase1l3*) gene.

RESULTS: Aberrations in the profile of plasma DNA jagged ends correlated with the type of nuclease that had been genetically deleted, depending on nucleosomal structures. The deletion of *Dnase1l3* led to a significant reduction of jaggedness for those plasma DNA molecules involving more than 1 nucleosome (e.g., size ranges 240-290 bp, 330-380 bp, and 420-470 bp). However, less significant effects of *Dnase1* and *Dffb* deletions were observed regarding different sizes of DNA fragments. Interestingly, the aberration in plasma DNA jagged ends related to multinucleosomes was observed in human subjects with familial systemic lupus erythematosus with *Dnase1l3* deficiency and human subjects with sporadic systemic lupus erythematosus.

CONCLUSIONS: Detailed understanding of the relationship between nuclease and plasma DNA jaggedness has opened up avenues for biomarker development.

There is an increasing interest in the roles of DNA nucleases in cell-free DNA (cfDNA) fragmentation (1–6). For instance, the deletion of *deoxyribonuclease 1 like 3* (*Dnase1l3*) leads to a striking reduction of plasma DNA molecules terminated with cytosine nucleotide (C-end) in mouse models (2, 4), thus establishing the relationship between DNASE1L3 and cfDNA fragmentation. One study explored other nucleases such as deoxyribonuclease 1 (DNASE1) and DNA fragmentation factor subunit beta (DFFB) by studying mice deficient in these nucleases (4). Other studies further demonstrated that plasma DNA end motifs represent a biomarker for patients with hepatocellular carcinoma (7, 8).

In addition to end motifs of cfDNA, one emerging fragmentomic feature is the jagged ends of plasma DNA (i.e., double-stranded plasma DNA molecules with protruding single-stranded ends) (9). Growing evidence suggests that the DNASE1 is one of the enzymes responsible for jagged end generation (9). In this regard, the jaggedness of urinary cfDNA has been shown to be

[a]Centre for Novostics, Hong Kong Science Park, Pak Shek Kok, New Territories, Hong Kong SAR, China; [b]Li Ka Shing Institute of Health Sciences, The Chinese University of Hong Kong, Shatin, New Territories, Hong Kong SAR, China; [c]Department of Chemical Pathology, The Chinese University of Hong Kong, Prince of Wales Hospital, Shatin, New Territories, Hong Kong SAR, China; [d]Clinica Pediatrica e Reumatologia, Centro per le malattie Autoinfiammatorie e Immunodeficienze, Istituto di Ricovero e Cura a Carattere Scientifico (IRCCS) Istituto Giannina Gaslini, Genova, Italy; [e]Dipartimento di Neuroscienze, Riabilitazione, Oftalmologia, Genetica e Scienze Materno-Infantili (DINOGMI), Università degli Studi di Genova, Genova, Italy; [f]Division of Rheumatology, The Hospital for Sick Children, Toronto, ON, Canada; [g]Department of Biomedical, Experimental and Clinical Sciences Mario Serio, University of Florence, Florence, Italy; [h]Medical Genetics Unit, Meyer Children's Hospital, Florence, Italy; [i]Nephrology and Dialysis Unit, Meyer Children's Hospital, Florence, Italy; [j]Nephrology Unit, University Hospital of Parma, Parma, Italy; [k]Department of Medicine and Therapeutics, The Chinese University of Hong Kong, Prince of Wales Hospital, Shatin, New Territories, Hong Kong SAR, China; [l]State Key Laboratory of Translational Oncology, The Chinese University of Hong Kong, Prince of Wales Hospital, Shatin, New Territories, Hong Kong SAR, China.
*Address correspondence to this author at: Department of Chemical Pathology, The University of Hong Kong, Prince of Wales Hospital, 30-32 Ngan Shing Street, Shatin, New Territories, Hong Kong SAR, China. Fax +85-226365090; e-mail: loym@cuhk.edu.hk.
[†]These authors contributed equally to this work.
Received November 11, 2021; accepted February 15, 2022.
https://doi.org/10.1093/clinchem/hvac050

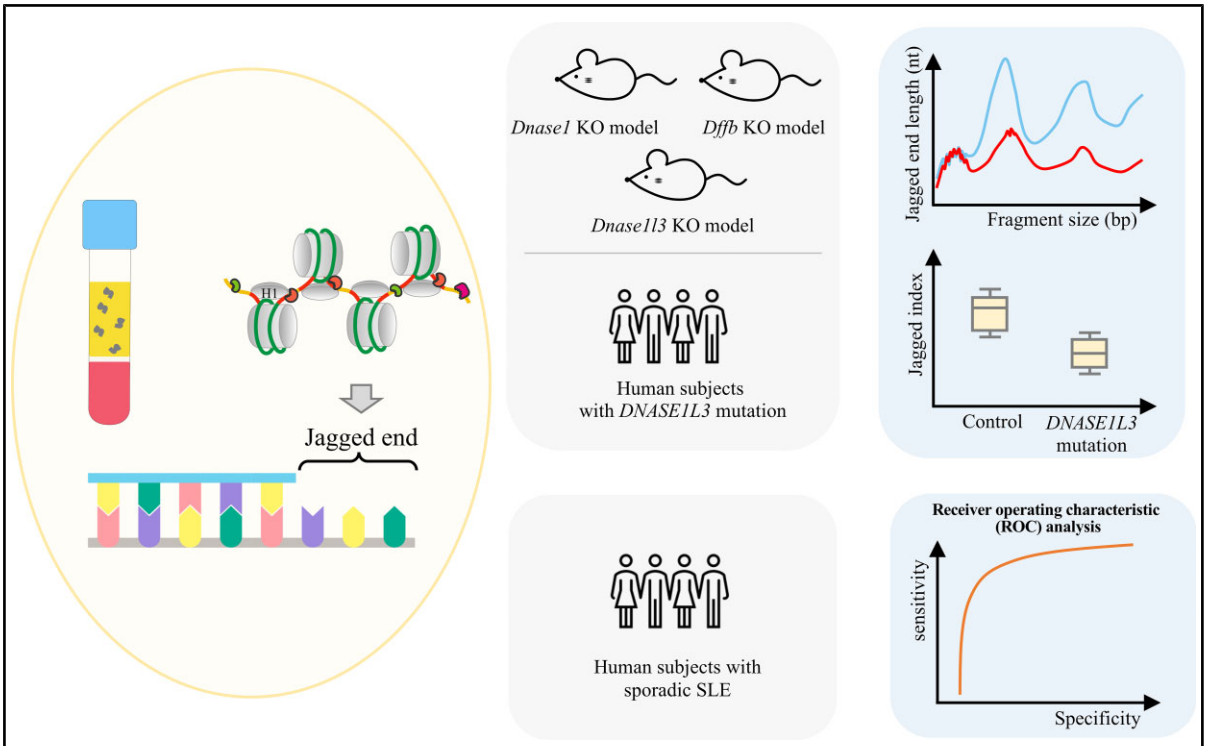

Fig. 1. Study design. cfDNA molecules would bear jagged ends resulting from nuclease cutting. Mouse models with *Dnase1*, *Dnase1l3*, or *Dffb* deletion were firstly used to explore the detailed relationship between jagged ends and nucleases based on jagged end length distribution. Human subjects carrying heterozygous or homozygous *DNASE1L3* mutation were studied to validate the utility of jaggedness in familial SLE. Receiver operating characteristic analysis was performed to assess the performance of jaggedness in discriminating patients with and without sporadic SLE.

higher than that of plasma DNA in humans due to the high DNASE1 activity in urine (10). However, much remains to be learned regarding the biology of the jaggedness of plasma DNA (e.g., the relationship between jaggedness and nucleosome structures). An improved understanding of plasma DNA jaggedness might spur clinical applications for disease detection and monitoring.

In this study, we investigated the jagged ends in plasma DNA of mice with *Dnase1*, *Dnase1l3*, or *Dffb* deletion in an effort to explore the detailed relationship between jaggedness and nucleases. We further investigated the plasma DNA jaggedness in human subjects with familial systemic lupus erythematosus (SLE) caused by DNASE1L3 deficiency and others with sporadic SLE (Fig. 1).

Material and Methods

HUMAN SAMPLE COLLECTION

We prospectively recruited 5 individuals from the Istituto Giannina Gaslini (Italy) and the Hospital for Sick Children (Canada) with written informed consent. This cohort involved 5 patients with *DNASE1L3* mutations, including 1 patient carrying a *DNASE1L3* mutation in a heterozygous state and 4 patients carrying homozygous *DNASE1L3* mutations. The study was approved by the Joint Chinese University of Hong Kong-Hospital Authority New Territories East Cluster Clinical Research Ethics Committee, the Ethics Committee of the Istituto Giannina Gaslini, and the Hospital for Sick Children Research Ethics Board.

MOUSE SAMPLE COLLECTION

Dnase1$^{-/-}$ mice (n = 7), *Dffb*$^{-/-}$ mice (n = 6), and their wild-type counterparts (*Dnase1*$^{+/+}$, n = 7; *Dffb*$^{+/+}$, n = 6) on C57BL/6 genomic background were obtained from the Knockout Mouse Project Repository of the University of California at Davis. *Dnase1l3*$^{-/-}$ mice
(n = 5) and their wild-type counterparts (*Dnase1l3*$^{+/+}$; n = 5) on C57BL/6 genomic background were custom-ordered from the Jackson Laboratory. All mice

were maintained in the Laboratory Animal Services Centre of The Chinese University of Hong Kong. These mice were acquired under a third-party distribution agreement and therefore were nontransferable. All experimental procedures were approved by the Animal Experimentation Ethics Committee of the Chinese University of Hong Kong.

SAMPLE PROCESSING

Mice were anesthetized and exsanguinated by cardiac puncture. Peripheral blood from human subjects was collected by venipuncture. Blood samples were immediately collected into EDTA-containing tubes and centrifuged at 1600 g for 10 min at 4°C. The plasma portion was further subjected to centrifugation at 16 000 g for 10 min at 4°C to pellet the residual cells and platelets. The resulting plasma was used for analysis (11). Plasma DNA was extracted with the QIAamp Circulating Nucleic Acid Kit (Qiagen) according to the manufacturer's protocol.

SAMPLE PREPARATION FOR JAG-SEQ

The jagged index or jagged end length of cfDNA was determined by DNA end-repair process to introduce different methylation signals between the original strand and the newly synthesized strand, named Jag-seq (9).

JAGGED INDEX ANALYSIS

DNA libraries for jagged index analysis were prepared with the KAPA HTP Library Preparation Kit (Roche) according to the manufacturer's protocol. The DNA libraries were then treated with bisulfite using an Epitect Plus Bisulfite kit (Qiagen). The bisulfite-treated DNA molecules were amplified using a KAPA HiFi HotStart Uracil + ReadyMix (Roche). PCR products were purified with a MinElute PCR purification kit (Qiagen). The fragment size of a plasma DNA sample was assessed by the Agilent 4200 tapestation system using the D1000 ScreenTape (Agilent). DNA sample quantity was measured by a Qubit Fluorometer (ThermoFisher Scientific). The ready-for-sequencing samples were then sequenced using a paired-end mode (75 bp × 2) on an Illumina HiSeq 4000 or NextSeq 500.

The incorporated unmethylated cytosines during the end-repair of jagged ends would decrease the methylation levels in CpG sites close to the 3' ends. The jaggedness of cfDNA molecules was measured by calculating the jagged index (i.e., $\frac{M1-M2}{M1} \times 100\%$, where $M1$ is the methylation density of read1 and $M2$ is the methylation density of read2) (9).

JAGGED END LENGTH ANALYSIS

DNA libraries for jagged end length analysis were constructed using a modified KAPA HTP Library Preparation Kit (Roche) (9). The modified protocol made use of Exo T (New England Biolabs) for removing 3' protruding ends and Klenow Fragment (exo-) (New England Biolabs) for the end-repair process with dATP (A), dGTP (G), dTTP (T), and methylated dCTP. The end-repaired DNA molecules carried A tails, facilitating the downstream sequencing adapter ligation. Polynucleotide kinase (New England Biolabs) was further used to phosphorylate the 5' end, and T4 ligase (New England Biolabs) was used to ligate index sequences (TruSeq DNA Single Index; Illumina) to the DNA library samples. A MinElute Reaction Cleanup Kit (Qiagen) was used for cleanup during the library preparation process. The DNA libraries were treated similarly as murine samples for bisulfite conversion, library amplification, purification, and quantitation.

The incorporated methylated cytosine during the end-repair of jagged ends would increase the methylation levels in CH sites close to the 3' ends. With the incorporation of methylated cytosines, we could calculate the exact length of the jagged end when the jagged end started at the second cytosine in a CC dinucleotide context (9). After bisulfite treatment, the first C from the original double-strand fragment would be converted to T. Since the second C was the first nucleotide incorporated into the new strand at the jagged end, the methylated cytosine incorporated would remain unchanged following bisulfite treatment. The conversion pattern of CC to TC would be used to mark the starting position of a jagged end, enabling the determination of the exact length of the jagged end.

SEQUENCING ALIGNMENT

Low-quality bases close to the 3' end in a sequencing direction were removed, and the sequencing adapters, if present in sequencing reads, were trimmed. The preprocessed reads in FASTQ format were then aligned to the mouse reference genome or human reference genome using methylation-aware aligners (12, 13), respectively. Only paired-end reads with read1 and read2 both aligned to the same chromosome in the correct orientation were used for downstream analyses. The spanning size between the read1 and read2 for each paired-end read was required to be ≤600 bp. All but one duplicated paired-end reads with identical start and end coordinates were removed.

PUBLICLY AVAILABLE BISULFITE SEQUENCING DATA SETS FOR JAGGED END ANALYSIS

Bisulfite sequencing data of plasma DNA of *Dnase1*$^{-/-}$ and *Dnase1l3*$^{-/-}$ mice were obtained from a published study (9). Bisulfite sequencing data of patients with active (n = 13) and inactive SLE (n = 11), as well as healthy controls (n = 10), were obtained from the

same cohort study previously published, for which the samples were recruited from Prince of Wales Hospital, Hong Kong (14).

Results

NUCLEOSOMAL STRUCTURES DEFINED BY CFDNA SIZE DISTRIBUTION

Previous studies revealed that periodic frequencies in cfDNA size distribution were reminiscent of distances between the nucleosome ladders observed in gel electrophoresis of DNA resolved from micrococcal nuclease digested chromatin (15). From the cfDNA size profile, plasma DNA molecules with sizes of 170 bp, 359 bp, and 550 bp were associated with mono-, di-, and trinucleosomes containing linker DNA at termini of the cfDNA molecules (Fig. 2). A nucleosome generally consists of a histone octamer wrapped with DNA molecules, an H1 linker histone associated linker DNA, and H1-free linker DNA (Fig. 2, B). For instance, hypothetically, a 170-bp DNA molecule might consist of 146-bp nucleosome core, approximately 20-bp H1-bound linker DNA, and 4-bp H1-free linker DNA (Fig. 2, C, i) (16, 17). A 359-bp DNA supposedly corresponded to two nucleosome cores ($146 \times 2 = 292$ bp), two H1-bound linker DNA segments (approximately $20 \times 2 = 40$ bp), 4-bp free linker DNA, and one H1-free linker DNA segment between two nucleosomes (approximately 23 bp) (Fig. 2, C, ii). In addition, 268-bp and 461-bp molecules would represent di- and trinucleosomes lacking the linker DNA at the termini (Fig. 2, C, iii and iv). For example, a 268-bp DNA molecule might derive from a 359-bp fragment with the H1-bound linker DNA segment trimmed off, followed by an extended trimming of 67 bp toward DNA molecules originally bound with the nucleosome core (Fig. 2, C, iii). A 461-bp fragment might originate

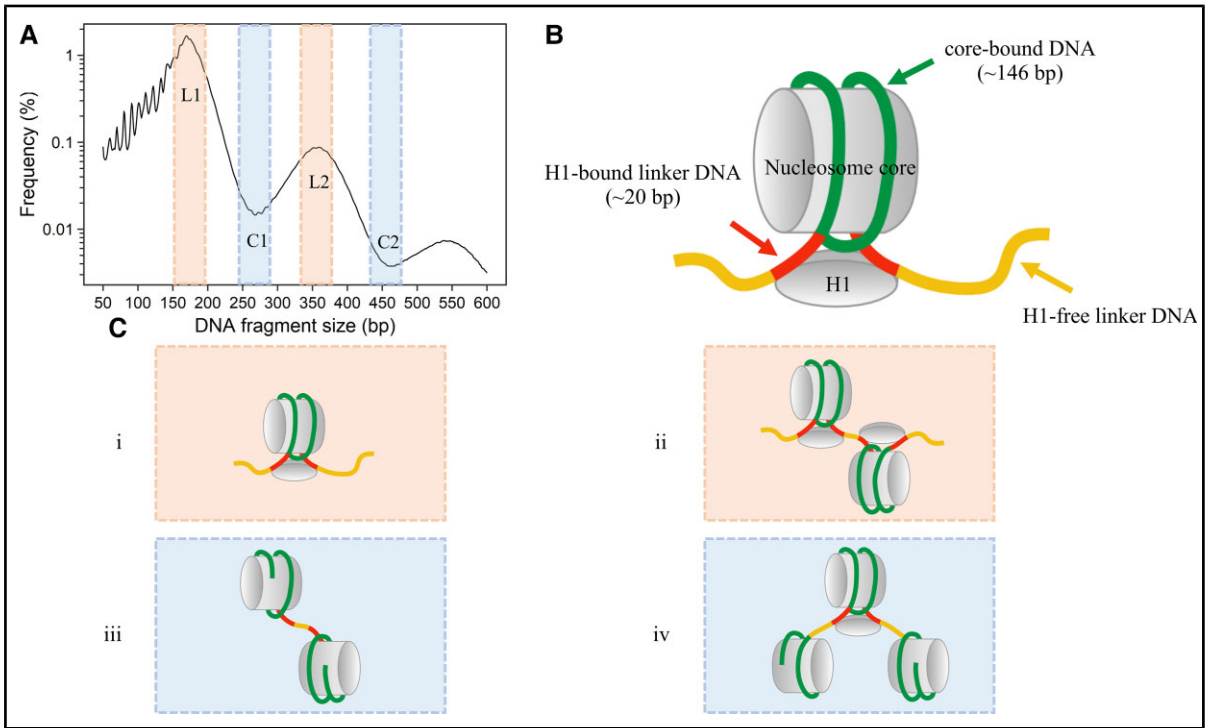

Fig. 2. Nucleosome structures defined by cfDNA size distribution. (A), Pooled size profile of wild-type mice with frequencies in logarithmic scale (y-axis). According to the peaks and troughs present in the size profile, we defined fragments with the size from 150 to 200 bp and 330 to 380 bp as cfDNA tailed with linker DNA (L1 and L2, shaded in orange), fragments with size from 240 to 290 bp and 420 to 470 bp as cfDNA lacking linker DNA tails (i.e., ending on nucleosomal core regions, C1 and C2, shaded in blue). (B), Model of nucleosome structures. A nucleosome consists of a nucleosome core that is composed of a histone octamer core, a histone H1, core-bound DNA molecules, H1-bound DNA molecules, and H1-free linker DNA. (C), i and ii, fragments tailed with linker DNA; iii and iv, fragments lacking linker DNA tails.

from a 550-bp fragment with the H1-bound linker DNA trimmed off, followed by the further trimming of 65-bp nucleosome core-related DNA molecules (Fig. 2, C, iv). According to the peaks and troughs present in the size profile, we defined fragments sized from 150 to 200 bp and 330 to 380 bp as cfDNA tailed with linker DNA (L1 and L2) and fragments sized from 240 to 290 bp and 420 to 470 bp as cfDNA lacking linker DNA tails (i.e., ending on nucleosomal core regions, C1 and C2) (Fig. 2, A). We further explored the relationship between the jagged end length of plasma DNA and the nucleosomal structures across mouse models in the following sections, by knocking out different nucleases.

JAGGED END LENGTHS OF CFDNA IN NUCLEASE DELETION MOUSE MODELS

Dnase1$^{-/-}$ *mouse model.* The median number of mapped paired-end reads was 30.0 million [interquartile range (IQR): 19.6–46.3 million]. We investigated the jaggedness of DNA fragments across a size range from 50 to 600 bp for mice with homozygous *Dnase1* deletion (*Dnase1*$^{-/-}$) on the basis of DNA end-repair process using methylated cytosines. For both homozygous *Dnase1* deletion (*Dnase1*$^{-/-}$) mice (n = 7) and their wild-type counterparts (n = 7), jagged end length distribution showed major peaks at 261 bp and 458 bp (Fig. 3, A). An overall decrease of jagged end length in *Dnase1*$^{-/-}$ mice (median: 25.2 nucleotides (nt); range: 23.2–28.5 nt) was observed when compared with wild-type mice (median: 27.0 nt; range: 25.0–28.0 nt). According to the nucleosome structures in detail (see online Supplementary Fig. 1, A), *Dnase1*$^{-/-}$ mice showed shorter jagged end lengths in L1, C1, L2, and C2. These results supported that DNASE1 would introduce jagged ends in both nucleosome core and linker DNA.

Dffb$^{-/-}$ *mouse model.* The median number of mapped paired-end reads was 73.3 million (IQR: 60.3–101.0 million). We analyzed the jaggedness of

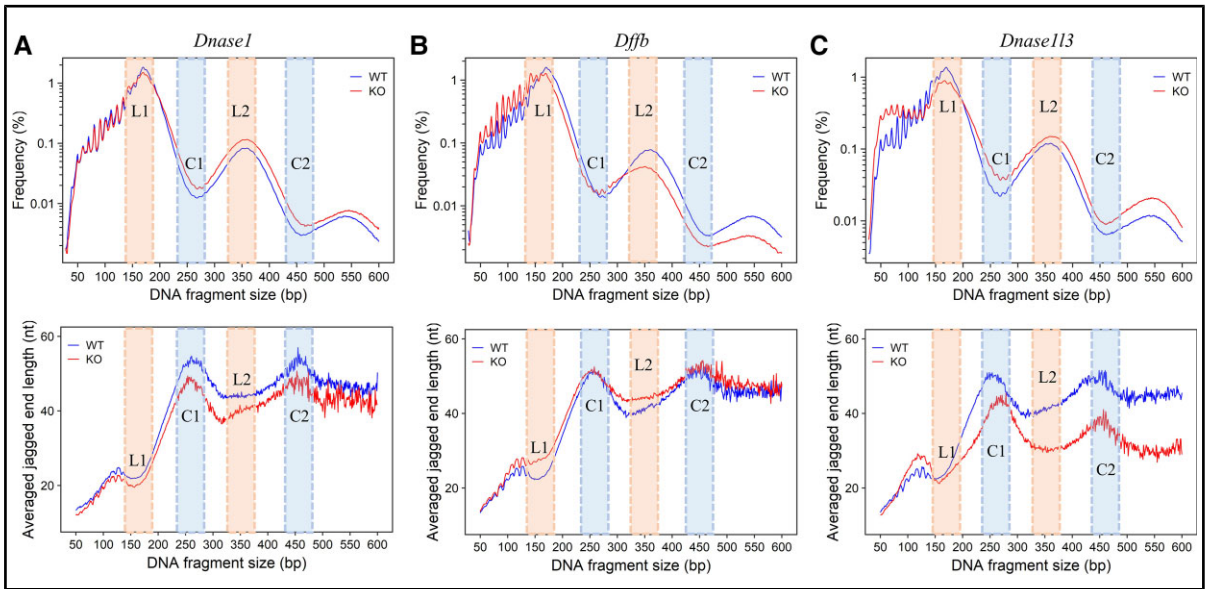

Fig. 3. Jagged end lengths of plasma DNA in mouse models with different nucleases deficiency. (A), Upper panel: Fragment size profile (in logarithmic scale) between mice with *Dnase1* deletion (red, n = 7) and wild-type counterparts (blue, n = 7), with annotations regarding L1 and L2 (shaded in orange), C1, and C2 (shaded in blue). Lower panel: Jagged end lengths across fragment sizes between mice with *Dnase1* deletion (red, n = 7) and wild-type counterparts (blue, n = 7). (B), Upper panel: Fragment size profile (in logarithmic scale) between mice with *Dffb* deletion (red, n = 6) and wild-type counterparts (blue, n = 6). Lower panel: Jagged end lengths across fragment size between mice with *Dffb* deletion (red, n = 6) and wild-type counterparts (blue, n = 6). (C), Upper panel: Fragment size profile (in logarithmic scale) between mice with *Dnase1l3* deletion (red, n = 5) and wild-type counterparts (blue, n = 5). Lower panel: Jagged end lengths across fragment sizes between mice with *Dnase1l3* deletion (red, n = 5) and wild-type counterparts (blue, n = 6). KO and WT represent the nuclease-deficient group and the corresponding wild-type group, respectively.

cfDNA across a size range from 50 to 600 bp for mice with homozygous *Dffb* deletion (*Dffb*$^{-/-}$). The jagged end length profile of homozygous *Dffb* deletion (*Dffb*$^{-/-}$) mice (n = 6) displayed a slight increase of jaggedness only in fragments tailed with linker DNA (Fig. 3, B) when compared with their wild-type counterparts (n = 6). *Dffb*$^{-/-}$ mice showed longer jagged end length in L1 and L2 while showing no significant difference in C1 and C2 (Supplementary Fig. 1B). These results supported that DFFB exhibited a preference in producing relatively shorter and/or blunt ends in fragments tailed with linker DNA.

Dnase1l3$^{-/-}$ *mouse model.* The median number of mapped paired-end reads was 30.3 million (IQR: 22.8–40.9 million). We compared the jagged end length distributions between homozygous *Dnase1l3* deletion (*Dnase1l3*$^{-/-}$) mice (n = 5) and their wild-type counterparts (n = 5) across a fragment size range of 50 to 600 bp. We observed significant differences in jaggedness between *Dnase1l3*$^{-/-}$ and wild-type mice at different fragment size ranges (Fig. 3, C). In contrast, the relatively small alterations were caused by the knocking out of *Dnase1* or *Dffb*. An increase of jaggedness was observed in fragments shorter than approximately 150 bp, while a more noticeable decrease of jaggedness was related to those fragments longer than approximately 200 bp. Those short fragments with a size below approximately 150 bp gave rise to a median 3.4% increase in jaggedness for *Dnase1l3*$^{-/-}$ mice, which was consistent with a previous report (9). For those long plasma DNA molecules >200 bp, a median 19.7% decrease in jagged end length was observed in *Dnase1l3*$^{-/-}$ mice (*P*-value <0.01, Mann-Whitney *U* test). Intriguingly, compared with wild-type mice, the deletion of *Dnase1l3* resulted in a significant reduction of jagged end length for those plasma DNA molecules involving multinucleosomes, *Dnase1l3*$^{-/-}$ mice displayed a decrease in L1, C1, L2, and C2 (Supplementary Fig. 1, C). These results supported that DNASE1L3 might have distinct effects on cfDNA jagged ends in association with nucleosomal structures. For example, DNASE1L3 exhibited a preference in introducing more jaggedness to multinucleosome-sized molecules rather than mononucleosome-sized molecules, and jaggedness would be more prominent when the DNA degradation involved the nucleosomal core regions.

Taken together, DNASE1, DFFB, and DNASE1L3 exhibited different properties in cfDNA fragmentation, characterized with different profiles of jagged ends. DNASE1 tended to generate jagged ends for a wide size spectrum of plasma DNA molecules, seemingly regardless of core and linker DNA. DFFB tended to generate relatively shorter and/or blunt jagged ends in linker DNA. DNASE1L3 preferentially introduced jagged ends on molecules related to multinucleosomes.

JAGGEDNESS OF CFDNA IN HUMAN SUBJECTS WITH *DNASE1L3* MUTATIONS

It has been reported that DNASE1L3-deficient mice develop autoantibodies to DNA and chromatin, followed by clinical features of SLE (18–20). In view of this, we studied whether the aberrations in jaggedness of plasma DNA present in *Dnase1l3*$^{-/-}$ mice could be mirrored in human patients with *DNASE1L3* mutations. To maximize jaggedness signals from multinucleosomes, we analyzed the jaggedness of fragments larger than 200 bp in 5 human subjects with *DNASE1L3* mutations and 10 healthy human subjects (14), using the bisulfite sequencing results (i.e., DNA end-repaired with unmethylated cytosines, followed by bisulfite sequencing), with a median of 128.8 million paired-end reads (IQR: 61.1–145.5 million). Subject H1 carried the heterozygous *DNASE1L3* mutation (i.e., one copy of the *DNASE1L3* gene being still functional). Subjects H2, H4, V11, and V12 carried homozygous *DNASE1L3* mutations (i.e., both copies of the *DNASE1L3* gene do not produce functional DNASE1L3 enzymes).

The extent of jagged index values in DNA molecules with sizes larger than 200 bp (median jagged index value: 21.7; range: 19.6–24.9) declined significantly in patients with homozygous *DNASE1L3* mutations (Fig. 4) compared with healthy controls (median jagged index value: 42.8; range: 37.5–45.6; *P*-value < 0.01) and the subject with heterozygous *DNASE1L3* variants (jagged index value: 38.1). The observation in the human subject with DNASE1L3 deficiency agreed with the observation from *Dnase1l3*$^{-/-}$ mice in which the *Dnase1l3* deletion led to a sharp decline of jaggedness in molecules with multinucleosomal sizes. Jagged index values appeared to be comparable between the subject with heterozygous *DNASE1L3* variants (jagged index value: 38.1) and healthy human controls (Fig. 4).

THE JAGGEDNESS OF CFDNA IN HUMAN SUBJECTS WITH SLE

We investigated whether such aberrations of jaggedness could serve as a biomarker for more common autoimmune diseases. To explore the potential clinical application, we used the jaggedness of molecules >200 bp in size, maximizing the jaggedness signals from multinucleosomes. We analyzed the bisulfite sequencing results of plasma DNA from a cohort of patients with sporadic SLE comprising 11 patients with inactive SLE, 13 patients with active SLE, and 10 healthy human subjects from a previous study (14). The end-repair step prior to the bisulfite conversion in this study was based on unmethylated cytosines. The SLE activity of the patients was based on the assessment of the Systemic Lupus Erythematosus Disease Activity Index (SLEDAI) (21).

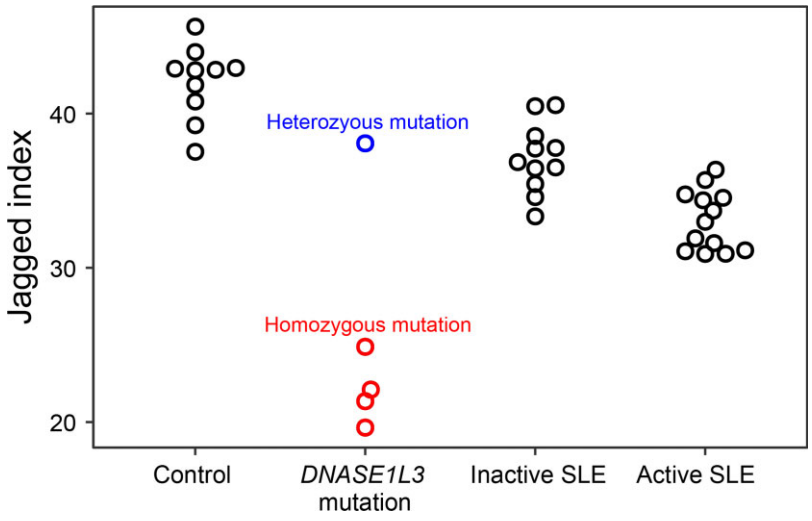

Fig. 4. The jaggedness of cfDNA in healthy human control subjects and patients with SLE. Boxplot shows jagged index values of plasma DNA over 200 bp among healthy human subjects (n = 10), patients with *DNASE1L3* mutation. Blue and red dots represent the subject carrying the heterozygous *DNASE1L3* mutation (n = 1) and subjects carrying the homozygous *DNASE1L3* mutation (n = 4) from the familial SLE group, respectively; black dots represent patients with inactive SLE (n = 11) or patients with active SLE (n = 13).

The jaggedness differed among the healthy human controls and patients with active and inactive SLE (Fig. 4). There was a median of 23.0% decrease in jaggedness for patients with active SLE (median jagged index value: 33.0; range: 30.9–36.4) relative to healthy human controls (median jagged index value: 42.8; range: 37.5–45.6; *P*-value <0.01, Mann-Whitney *U* test). For those patients with inactive SLE (median jagged index value: 36.9; range: 33.3–40.5), the median jaggedness was 14.0% lower than healthy human controls (*P*-value <0.01, Mann-Whitney *U* test) (Fig. 4), but 11.7% higher than those with active SLE. These data supported that the change of jaggedness would correlate with SLE activity. We performed a ROC curve analysis to assess the discriminative power of jagged ends in differentiating patients with active SLE from patients without active SLE. The area under the ROC curve (AUC) was 0.96 between subjects with active SLE and those subjects without active SLE (i.e., patients with inactive SLE and healthy human subjects) (Fig. 5). In addition, the AUC was 0.94 between patients with inactive SLE and healthy human subjects (Fig. 5). More important, the jaggedness of plasma DNA enabled the classification between patients with active SLE and inactive SLE (AUC: 0.92) (Fig. 5), supporting the feasibility of using jagged ends to monitor changes in SLE disease activity. The jaggedness of plasma DNA in patients with SLE correlated with the SLEDAI (Fig. 6) (Pearson's r: −0.69; *P*-value <0.01). The data further supported the conclusion that the jaggedness aberrations could be reflective of flares of SLE.

Discussion

In this study, we investigated the relationship between plasma DNA jaggedness and 3 nucleases (i.e., DNASE1, DFFB, and DNASE1L3) reported to be involved in cfDNA fragmentation (3, 4, 18, 22). Our data demonstrates that DNASE1, DFFB, and DNASE1L3 might have different roles in determining the profiles of jagged ends. DNASE1L3 had a distinct role in generating jagged ends and preferentially introduced jagged ends on molecules related to multinucleosomes. In contrast, DNASE1 might generate jagged ends across plasma DNA molecules in a wide size range, seemingly exhibiting less significant preference relative to the nucleosome structures. DFFB would preferentially generate relatively shorter and/or blunt jagged ends in linker DNA.

One previous study focused on the jaggedness for those molecules within a size range of 130 to 160 bp that would be derived from the degradation of mononucleosome-sized fragments. An increased jaggedness was observed in the plasma of *Dnase1l3*$^{-/-}$ mice

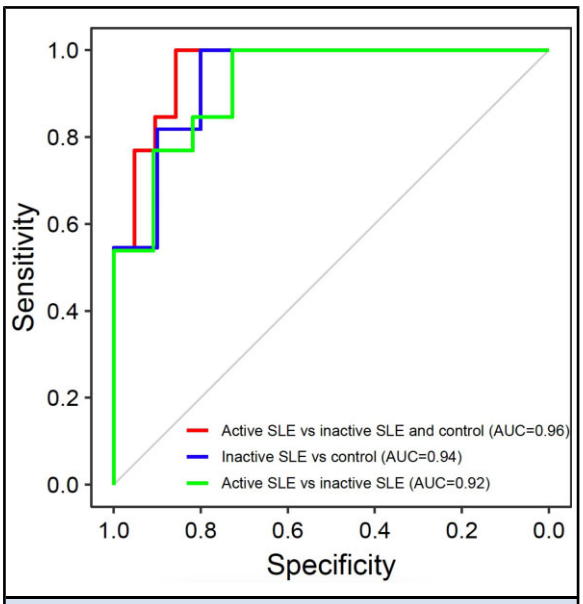

Fig. 5. The discriminative power of jaggedness in differentiating between patients with and without active SLE. The red ROC curve demonstrates the differentiation between patients with active SLE vs healthy human subjects and patients with inactive SLE based on the parameter of plasma DNA jagged end index. The blue ROC curve demonstrates the differentiation between patients with inactive SLE vs healthy subjects. The green ROC curve demonstrates the differentiation between patients with active SLE versus patients with inactive SLE.

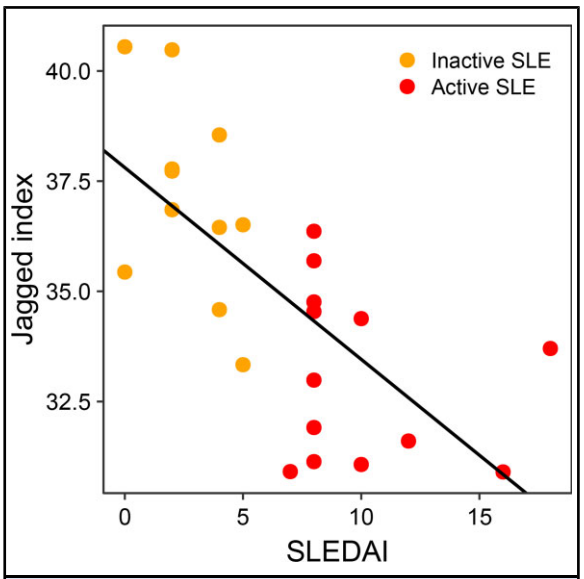

Fig. 6. Correlation between the Systemic Lupus Erythematosus Disease Activity Index (SLEDAI) and jagged index in patients with inactive SLE or active SLE. Orange dots indicate patients with inactive SLE; red dots indicate patients with active SLE.

(9). In this study, we observed more pronounced changes in an opposite direction occurring at those DNA molecules with multinucleosome sizes in mice with *Dnase1l3* deletion. In contrast to the less significant effects of *Dnase1* and *Dffb* deletions, the deletion of *Dnase1l3* would lead to a significant reduction of jaggedness for those plasma DNA molecules involving multinucleosomes (e.g., size ranges: 240–290 bp, 330–380 bp, and 420–470 bp). Such size ranges were previously given less attention by investigators in the field, partly because of the much lower abundance in terms of molecule numbers within multinucleosome-sized ranges (16.5% for wild-type mice, 2.9% for healthy human subjects) than that of fragments with size range related to mononucleosome (83.5% for wild-type mice, 97.1% for healthy human subjects). Enhanced effects of DNASE1L3 found in fragments involving multinucleosome sizes might be in part be due to the nature of DNASE1L3 that was highly effective in digesting chromatins (23–25).

Another previous study covered the jaggedness distribution corresponding to nucleosomal structure (10). The authors speculated that jaggedness might be relatively enriched in linker DNA when aligning plasma DNA fragments to the nucleosome arrays obtained from micrococcal nuclease-sequencing data (26) using all plasma DNA molecules without in silico size fractionation. The jaggedness signal would predominantly reflect the characteristics of molecules with 166 bp, which are most abundant in plasma. Our work further investigated the jaggedness distribution within fragments of different sizes and demonstrated that the enzymatic digestion towards nucleosomal cores would introduce more jaggedness when focusing on another subset of plasma DNA molecules with 261 bp (i.e., dinucleosome peak [359 bp] with the removal of linker DNA [20 bp] plus extra removal of DNA in the nucleosomal core [78 bp]) than the molecules with 166 bp (i.e., mononucleosome peak [166 bp] containing linker DNA). It would be of value to study the jagged ends in nuclei digested by different nucleases.

DNASE1L3-deficient mice have been reported to develop an SLE-like disease (18, 27). The jaggedness aberrations observed in multinucleosome-sized fragments in *Dnase1l3*$^{-/-}$ mice could be phenotypically mirrored in the plasma DNA of human subjects with DNASE1L3 deficiency, demonstrating DNASE1L3 to be an important enzyme involving the generation of jagged ends in those plasma DNA molecules > 200 bp. Interestingly, such jaggedness not only attained a

significant difference between wild-type and *Dnase1l3*$^{-/-}$ mice but might also enable the differentiation between patients with and without sporadic SLE (AUC: 0.96). The use of mouse models and the size-selected subset of plasma DNA molecules may provide a strategy for future biomarker development regarding autoimmune or other diseases.

The jaggedness aberrations in patients with sporadic SLE might be due to multifaceted intracellular and extracellular factors. A recent study suggested that the DNASEL1L3 activity was impaired by the presence of autoantibody in patients with SLE having renal involvement (28). In that study, the DNASE1L3 activity was measured according to the digestion rate of double-stranded nuclei DNA derived from Jurkat T cells by the diluted human plasma (i.e., extracellular level), assuming that DNASEL1L3 acted on nuclei DNA far more efficient than DNASE1 (28). In addition to the impaired extracellular DNASE1L3 activity, the DNASE1L3 expression level in whole blood cells was significantly downregulated in patients with SLE compared with subjects without SLE (29), which might potentially downregulate the intracellular DNASE1L3 activity.

Taken together, plasma DNA jagged ends represent an emerging member of fragmentomic markers, providing possibilities for the detection and/or monitoring of autoimmune diseases. A detailed understanding between plasma DNA fragmentations and nuclease activities could spur the development of novel diagnostic tools.

Data Availability

Raw sequencing data of humans were submitted to European Genome-Phenome Archive (EGA), https://www.ebi.ac.uk/ega/, with the accession number of EGAS00001005562. Raw sequencing data of mice were submitted to European Genome-Phenome Archive (EGA), https://www.ebi.ac.uk/ega/, with the accession number of EGAS00001005563. The programming codes for the bioinformatics pipeline for detecting the jagged ends were publicly available as described in our previous study (9).

Supplemental Material

Supplemental material is available at *Clinical Chemistry* online.

Nonstandard Abbreviations: cfDNA, cell-free; DNASE1L3, deoxyribonuclease 1 like 3; DNASE1, deoxyribonuclease 1; DFFB, DNA fragmentation factor subunit beta; SLE, systemic lupus erythematosus; IQR, interquartile range; nt, nucleotides; ROC, receiver operating characteristic; AUC, area under the ROC curve; SLEDAI, Systemic Lupus Erythematosus Disease Activity Index.

Author Contributions: *All authors confirmed they have contributed to the intellectual content of this paper and have met the following 4 requirements: (a) significant contributions to the conception and design, acquisition of data, or analysis and interpretation of data; (b) drafting or revising the article for intellectual content; (c) final approval of the published article; and (d) agreement to be accountable for all aspects of the article thus ensuring that questions related to the accuracy or integrity of any part of the article are appropriately investigated and resolved.*

S.C. Ding, R.W.Y. Chan, P. Jiang, K.C.A. Chan, and Y.M.D. Lo designed the research. S.C. Ding and R.W.Y. Chan performed the experiments. W. Peng, L. Huang, Z. Zhou, X. Hu, and P. Jiang performed bioinformatics data analysis. S.C. Ding, R.W.Y. Chan, P. Jiang, R.W.K. Chiu, K.C.A. Chan, and Y.M.D. Lo wrote the manuscript. S. Volpi, L.T. Hiraki, L.-S. Tam, P.C.H. Wong, and L.H.P. Tam recruited clinical samples and interpreted clinical data. S.C. Ding, R.W.Y. Chan, P. Jiang, R.W.K. Chiu, K.C.A. Chan, and Y.M.D. Lo reviewed and interpreted the data.

Authors' Disclosures or Potential Conflicts of Interest: *Upon manuscript submission, all authors completed the author disclosure form. Disclosures and/or potential conflicts of interest:*

Employment or Leadership: R.W.K. Chiu, *Clinical Chemistry*, AACC; Y.M.D. Lo, *Clinical Chemistry*, AACC. Y.M.D. Lo is a scientific co-founder of Grail and has leadership or fiduciary role in Take2, DRA, and Centre for Novostics. K.C.A. Chan is a director of DRA, Take2, and Centre for Novostics. P. Jiang is a Director of DRA and KingMed Future. R.W.K. Chiu, Board of DRA, Board of Take2, and Secretary of International Society of Prenatal Diagnosis.
Consultant or Advisory Role: P. Jiang, K.C.A. Chan, R.W.K. Chiu, and Y.M.D. Lo were consultants to Grail; R.W.K. Chiu is a consultant to Illumina; P. Jiang is a consultant to Take2 and KMF.
Stock Ownership: K.C.A. Chan, R.W.K. Chiu, and Y.M.D.L. hold equities in DRA, Take2, and Grail/Illumina; P. Jiang holds equities in Grail/Illumina, DRA, and Take2.
Honoraria: L.T. Hiraki, Novartis, National Institutes of Health (NIH); R.W.K. Chiu, Illumina. K.C.A. Chan received travel support from BioRad.
Research Funding: This work was supported by the Research Grants Council of the Hong Kong Special Administrative Region (SAR) Government under the Theme-Based Research Scheme (T12-401/16-W), the Innovation and Technology Commission (*InnoHK* Initiative), and the Vice Chancellor's One-Off Discretionary Fund of the Chinese University of Hong Kong (VCF2014021). Y.M.D. Lo is supported by an endowed chair from the Li Ka Shing Foundation. K.C.A. Chan, R.W.K. Chiu, and Y.M.D. Lo previously received research funding from Grail via a collaborative research agreement. L.T. Hiraki, Canadian Institute of Health Research (CIHR), The Arthritis Society (TAS), and Lupus Research Alliance (LRA).
Expert Testimony: None declared.
Patents: S.C. Ding, R.W.Y. Chan, W. Peng, P. Jiang, K.C.A. Chan, R.W.K. Chiu, and Y.M.D.L. have filed patent applications based on the data generated from this work. Patent royalties are received from Grail, Illumina, Sequenom, DRA, Take2 Health, and Xcelom.

Role of Sponsor: The funding organizations played no role in the design of study, choice of enrolled patients, review and interpretation of data, preparation of manuscript, or final approval of manuscript.

Acknowledgments: We thank Daniela Dominguez for coordinating the transfer of human samples. We also thank Wing Shan Lee, Yongjie Jin, Huimin Shang for technical assistance.

References

1. Cheng THT, Lui KO, Peng XL, Cheng SH, Jiang P, Chan KCA, et al. Dnase1 does not appear to play a major role in the fragmentation of plasma DNA in a knockout mouse model. Clin Chem 2018;64:406–8.
2. Serpas L, Chan RWY, Jiang P, Ni M, Sun K, Rashidfarrokhi A, et al. Dnase1l3 deletion causes aberrations in length and end-motif frequencies in plasma DNA. Proc Natl Acad Sci U S A 2019;116:641–9.
3. Watanabe T, Takada S, Mizuta R. Cell-free DNA in blood circulation is generated by dnase1l3 and caspase-activated dnase. Biochem Biophys Res Commun 2019;516: 790–5.
4. Han DSC, Ni M, Chan RWY, Chan VWH, Lui KO, Chiu RWK, et al. The biology of cell-free DNA fragmentation and the roles of dnase1, dnase1l3, and dffb. Am J Hum Genet 2020;106:202–14.
5. Lo YMD, Han DSC, Jiang P, Chiu RWK. Epigenetics, fragmentomics, and topology of cell-free DNA in liquid biopsies. Science 2021;372:eaaw3616.
6. Han DSC, Lo YMD. The nexus of cfdna and nuclease biology. Trends Genet 2021;37: 758–70.
7. Jiang P, Sun K, Peng W, Cheng SH, Ni M, Yeung PC, et al. Plasma DNA end motif profiling as a fragmentomic marker in cancer, pregnancy and transplantation. Cancer Discov 2020;10:664–73.
8. Chen L, Abou-Alfa GK, Zheng B, Liu JF, Bai J, Du LT, et al. Genome-scale profiling of circulating cell-free DNA signatures for early detection of hepatocellular carcinoma in cirrhotic patients. Cell Res 2021;31:589–92.
9. Jiang P, Xie T, Ding SC, Zhou Z, Cheng SH, Chan RWY, et al. Detection and characterization of jagged ends of double-stranded DNA in plasma. Genome Res 2020;30:1144–53.
10. Zhou Z, Cheng SH, Ding SC, Heung MMS, Xie T, Cheng THT, et al. Jagged ends of urinary cell-free DNA: Characterization and feasibility assessment in bladder cancer detection. Clin Chem 2021;67:621–30.
11. Chiu RW, Poon LL, Lau TK, Leung TN, Wong EM, Lo YM. Effects of blood-processing protocols on fetal and total DNA quantification in maternal plasma. Clin Chem 2001;47:1607–13.
12. Xi Y, Li W. Bsmap: Whole genome bisulfite sequence mapping program. BMC Bioinformatics 2009;10:232.
13. Jiang P, Sun K, Lun FM, Guo AM, Wang H, Chan KC, et al. Methy-pipe: an integrated bioinformatics pipeline for whole genome bisulfite sequencing data analysis. PLoS One 2014;9:e100360.
14. Chan RW, Jiang P, Peng X, Tam LS, Liao GJ, Li EK, et al. Plasma DNA aberrations in systemic lupus erythematosus revealed by genomic and methylomic sequencing. Proc Natl Acad Sci U S A 2014;111: E5302–11.
15. Chereji RV, Bryson TD, Henikoff S. Quantitative mnase-seq accurately maps nucleosome occupancy levels. Genome Biol 2019;20:198.
16. Cutter AR, Hayes JJ. A brief review of nucleosome structure. FEBS Lett 2015; 589(Pt A):2914–22.
17. Thomas JO. Histone h1: Location and role. Curr Opin Cell Biol 1999;11:312–7.
18. Sisirak V, Sally B, D'Agati V, Martinez-Ortiz W, Ozcakar ZB, David J, et al. Digestion of chromatin in apoptotic cell microparticles prevents autoimmunity. Cell 2016;166: 88–101.
19. Ozcakar ZB, Foster J, Diaz-Horta O, Kasapcopur O, Fan YS, Yalcinkaya F, et al. Dnase1l3 mutations in hypocomplementemic urticarial vasculitis syndrome. Arthritis Rheum 2013;65:2183–9.
20. Al-Mayouf SM, Sunker A, Abdwani R, Abrawi SA, Almurshedi F, Alhashmi N, et al. Loss-of-function variant in dnase1l3 causes a familial form of systemic lupus erythematosus. Nat Genet 2011;43: 1186–8.
21. Petri M, Orbai AM, Alarcon GS, Gordon C, Merrill JT, Fortin PR, et al. Derivation and validation of the systemic lupus international collaborating clinics classification criteria for systemic lupus erythematosus. Arthritis Rheum 2012;64:2677–86.
22. Keyel PA. Dnases in health and disease. Dev Biol 2017;429:1–11.
23. Mizuta R, Araki S, Furukawa M, Furukawa Y, Ebara S, Shiokawa D, et al. Dnase gamma is the effector endonuclease for internucleosomal DNA fragmentation in necrosis. PLoS One 2013;8:e80223.
24. Napirei M, Ludwig S, Mezrhab J, Klockl T, Mannherz HG. Murine serum nucleases–contrasting effects of plasmin and heparin on the activities of dnase1 and dnase1-like 3 (dnase1l3). FEBS J 2009;276:1059–73.
25. Wilber A, Lu M, Schneider MC. Deoxyribonuclease I-like III is an inducible macrophage barrier to liposomal transfection. Mol Ther 2002;6:35–42.
26. Gaffney DJ, McVicker G, Pai AA, Fondufe-Mittendorf YN, Lewellen N, Michelini K, et al. Controls of nucleosome positioning in the human genome. PLoS Genet 2012;8:e1003036.
27. Soni C, Perez OA, Voss WN, Pucella JN, Serpas L, Mehl J, et al. Plasmacytoid dendritic cells and type I interferon promote extrafollicular B cell responses to extracellular self-DNA. Immunity 2020;52: 1022–38.e7.
28. Hartl J, Serpas L, Wang Y, Rashidfarrokhi A, Perez OA, Sally B, et al. Autoantibody-mediated impairment of dnase1l3 activity in sporadic systemic lupus erythematosus. J Exp Med 2021;218:e20201138.
29. Balci MA, Atli E, GüRkan H. Investigation of genes associated with atherosclerosis in patients with systemic lupus erythematosus. Arch Rheumatol 2021;36:287–95.